Published in final edited form as:
Acta Biomater. 2010 July ; 6(7): 2740–2750. doi:10.1016/j.actbio.2009.12.052.

Functional biomimetic analogs help remineralize apatite-depleted demineralized resin-infiltrated dentin via a bottom-up approach

Jongryul Kim[a], **Dwayne D. Arola**[b], **Lisha Gu**[c], **Young Kyung Kim**[d], **Sui Mai**[c], **Yan Liu**[e], **David H. Pashley**[f], and **Franklin R. Tay**[f,*]

[a] Department of Conservative Dentistry, School of Dentistry, Kyung Hee University, 1 Hoegi-dong, Dongdaemun-gu, Seoul, 130-701, South Korea

[b] Department of Mechanical Engineering, University of Maryland, 1000 Hilltop Circle, Baltimore, MD, 21250, USA

[c] Department of Operative Dentistry and Endodontics, Guanghua School of Stomatology, Sun Yat-sen University, 56 Lingyuan Road West, Guangzhou, 510055, China

[d] Department of Conservative Dentistry, School of Dentistry, Kyungpook National University Samduk-dong 2-ga, Jung-gu, Daegu, 700-412, South Korea

[e] Department of Stomatology, Tongji Hospital, Huazhong University of Science and Technology, Wuhan, China

[f] Department of Oral Biology, School of Dentistry, Medical College of Georgia, 1120, 15th Street, CL 2120, Augusta, GA, 30912-1129, USA

Abstract

Natural biominerals are formed through metastable amorphous precursor phases via a bottom-up, nanoparticle-mediated mineralization mechanism. Using an acid-etched human dentin model to create a layer of completely-demineralized collagen matrix, a bio-inspired mineralization scheme has been developed based on the use of dual biomimetic analogs. These analogs help to sequester fluidic amorphous calcium phosphate nanoprecursors and function as templates for guiding homogeneous apatite nucleation within the collagen fibrils. By adopting this scheme for remineralizing adhesive resin-bonded, completely-demineralized dentin, we have been able to redeposit intrafibrillar and extrafibrillar apatites in completely-demineralized collagen matrices that are imperfectly infiltrated by resins. This study utilizes a spectrum of completely- and partially-demineralized dentin collagen matrices to further validate the necessity for using a biomimetic analog-containing medium for remineralizing resin-infiltrated partially-demineralized collagen matrices in which remnant seed crystallites are present. In control specimens in which biomimetic analogs are absent from the remineralization medium, remineralization could only be seen in partially-demineralized collagen matrices probably by epitaxial growth via a top-down crystallization approach. Conversely, in the presence of biomimetic analogs in the remineralization medium, intrafibrillar remineralization of completely-demineralized collagen matrices via a bottom-up crystallization mechanism can additionally be identified. The latter is characterized by the transition of intrafibrillar minerals from an inchoate state of continuously-braided microfibrillar electron-dense

[*]Corresponding Authors: Department of Endodontics, School of Dentistry, Medical College of Georgia, 1120, 15th Street, CL 2132, Augusta, GA, 30912-1129, USA, Tel.: +1 706 721 2033; Fax: +1 706 721 6252; ftay@mail.mcg.edu (Franklin R. Tay).

amorphous strands to discrete nanocrystals, and ultimately into larger crystalline platelets within the collagen fibrils. Biomimetic remineralization via dual biomimetic analogs has the potential to be translated into a functional delivery system for salvaging failing resin-dentin bonds.

Keywords

collagen; dentin; intrafibrillar; remineralization; self-etching adhesive

1. Introduction

Dental caries is a transmittable infectious disease which represents pathologic destruction of hard and soft dental tissues by oral microorganisms. It affects individuals of all age, culture and socioeconomic background and is a major problem in dentistry despite significant advances in the development of preventive strategies over the past few decades [1]. Acids produced by cariogenic microorganisms diffuse through calcified dental tissues and result in dissolution of the apatite crystallites. Dental caries may be initiated from either the crown enamel or the root cementum and eventually progresses to the underlying dentin. Bacteria produce lactic acid until the local pH reaches about 4.5–5.0 at which time they cease to form any more lactic acid. The lactic acid tends to preferentially dissolve some, but not all, interfibrillar crystallites, creating a zone of partially demineralized dentin. The process also activates endogenous collagenolytic enzymes known as matrix metalloproteinases (MMPs) that break down the demineralized collagen matrix. Dentin contains approximately 70 wt% mineral phase, 20 wt % organic phase and 10 wt% water [2]. Type I collagen constitutes 90 wt% of the dentin organic phase and the remaining 10% is composed of noncollagenous proteins (NCPs) [3]. If demineralization by bacterial acids is not halted or reversed by re-deposition of minerals derived from salivary secretions, a cavity forms that requires replacement with a dental filling [1]. Contemporary management of caries has progressed historically from extraction of the caries-involved tooth to the use of minimally-invasive techniques that maximize the conservation of tooth structures. Filling of carious teeth with tooth-colored resin composites that are coupled to the dentin substrate via the use of dentin adhesives is the current treatment of choice.

Dentin adhesives rely on micromechanical entanglement of resin polymers within partially or completely-demineralized collagen matrices for retention of the resin composite fillings. Infiltration of resins into the demineralized dentin creates a so-called interdiffusion zone. Demineralization of dentin substrates for the sake of micromechanical retention may be accomplished by a separate phosphoric acid-etching step in the so-called etch-and-rinse adhesives or by utilizing acidic resin monomers with carboxylic acid or phosphoric acid functional groups in the so-called self-etching adhesives. When 37% phosphoric acid is used, the pH of the etched surface can fall below pH 1.0. At such low pHs, apatite crystallites are dissolved from both interfibrillar and intrafibrillar compartments, leaving the type I collagen completely demineralized. Conversely, when milder formers of self-etching adhesives are used, zones of partially demineralized dentin that contain seed apatite crystallites are produced. Resin-dentin bonds created by contemporary dentin adhesives are susceptible to degradation *in vivo* after aging [4–6] by endogenous MMPs that are bound to the demineralized collagen fibrils [7]. A potential strategy to improve the durability of these bonds is to replace the residual water trapped within the non-resin encapsulated demineralized collagen fibrils by new apatitic minerals. The newly formed apatitic minerals probably fossilize the MMPs and prevent the collagen fibrils from enzymatic degradation. This protection concept is based on the rationale that natural mineralized dentin that is protected by intrafibrillar and extrafibrillar apatite crystallites do not undergo degradation over time [8]. Since collagen matrix does not initiate mineralization on its own [9], noncollagenous extracellular matrix proteins are required for

regulating bone and dentin mineralization and for controlling the dimension, order and hierarchy of apatite deposition within mineralized hard tissues [10]. As the therapeutic use of native or recombinant ECM proteins for *in-situ* biomineralization is not yet economically viable, research scientists have resorted to the use of polyelectrolyte and poly(amino) acid macromolecules to mimic the functional domains of these naturally occurring proteins [11].

Most of the techniques involved in the synthesis of nanomaterials and nanodevices may be classified as bottom-up and top-down approaches [12]. Bottom-up approaches start with one or more defined molecular species, which undergo certain processes that result in a higher-ordered and highly-organized structure. Examples of bottom-up approaches include self-assembly and molecular patterning. Top-down approaches begin with a bulk material that incorporates nanoscale details, such as nanolithography and etching techniques. In the top-down approach, biomaterials are generated by stripping down a complex entity into its component parts, such as paring of a virus particle down to its capsid to form a viral cage. In terms of crystallization, creating smaller crystals from larger crystals in partially demineralized dentin by the aforementioned bacterial acids and self-etching primers represents examples of the top-down approach.

A nanotechnology-inspired, biomimetic mineralization technique that generates calcium and phosphate ions with a high pH has recently been developed [13]. This biomimetic mineralization scheme uses two polyanionic analogs to mimic the dual functions of dentin matrix proteins [14] in sequestering and stabilizing amorphous nanoprecursors that are generated from prenucleation clusters [15–17], and acting as template molecules [18,19] for guiding the bottom-up assembly [20] of intrafibrillar apatite crystallites within the collagen fibrils. The aforementioned biomimetic mineralization scheme has been adopted for remineralization of imperfect, water permeable resin-dentin interfaces created by etch-and-rinse dentin adhesives that utilize an aggressive phosphoric acid etchant to create a zone of completely-demineralized dentin on top of a mineralized dentin base [21,22]. The results derived from this completely-demineralized, resin-infiltrated dentin model led to the conclusion that intrafibrillar remineralization of water-rich, resin-sparse collagen matrices can not occur in the presence of a remineralization medium that is devoid of biomimetic analogs. The idea of dentin remineralization is certainly not new; the dental literature abounds with studies on a plethora of filling materials that are capable of remineralizing partially-demineralized dentin. An obvious difference between completely- and partially-demineralized dentin is the presence of remnant apatite seed crystallites in the latter that can act as centers for heterogeneous nucleation. Thus, remineralization of a partially-demineralized collagen matrix is thermodynamically more favorable than homogeneous nucleation within a completely-demineralized collagen matrix. Part of the success reported with the use of contemporary calcium- and phosphate-releasing remineralizing materials may be related to the remineralization of the collagen matrix via epitaxial growth of calcium phosphate salts on remnant seed crystallites [23]. Epitaxial growth may be regarded as a top-down approach according to the classical crystallization theory, via ion-by-ion addition to pre-existing seed crystallites [14]. Conversely, the bottom-up mineralization approach is based on the nonclassical theory of crystallization which involves the use of biomimetic analogs for generating metastable amorphous mineral precursors and mesocrystals. As a partially-demineralized collagen matrix invariably exhibits a gradient of demineralization from the surface to the base of the matrix, it is unknown if the aforementioned biomimetic analogs are required for remineralizing partially-demineralized collagen matrices. Intrafibrillar remineralization, in particular, has been surmised to be responsible for restoring the mechanical properties of dentin [24].

Unlike etch-and-rinse adhesives, self-etching adhesives contain polymerizable, methacrylate-based acidic resin monomers that simultaneously etch and infiltrate the dentin substrate. They

vary widely in their aggressiveness and may create completely- or partially-demineralized collagen matrices of variable thickness [25]. The use of hydrophilic self-etching adhesives of variable aggressiveness provides the opportunity for designing a phenomenological model consisting of a spectrum of completely- and partially-demineralized collagen matrices for validating the necessity of using a biomimetic analog-containing medium for remineralization of partially-demineralized dentin. Thus, the objective of this work was to examine the ultrastructural characteristics of completely-demineralized vs partially-demineralized resin-infiltrated dentin collagen matrices (i.e. interdiffusion zones) that had been subjected to biomimetic remineralization. Understanding the ultrastructural differences between top-down and bottom-up approaches in their ability to remineralize partially-demineralized resin-infiltrated dentin sets the stage for the development of the current biomimetic remineralization strategy as a functional delivery system for remineralizing partially-demineralized, resin-bonded caries-affected dentin.

2. Materials and methods

2.1 Dentin bonding

Twenty-four extracted non-carious human third molars were used for the study. The teeth were collected after the parents' informed consents were obtained under a protocol reviewed and approved by the Human Assurance Committee of the Medical College of Georgia. A flat dentin surface was prepared perpendicular to the longitudinal axis of each tooth using a low-speed Isomet diamond saw (Buehler Ltd., Lake Bluff, IL, USA) under water-cooling. The occlusal dentin surface was polished with a 320-grit silicon carbide paper under running water to create a bonding surface that was devoid of enamel. The specimens were randomly divided into three groups (8 teeth each): I) Adper Prompt (3M ESPE, St. Paul, MN, USA), the most aggressive self-etching adhesive; II) Adper Scotchbond SE (3M ESPE), a moderately aggressive self-etching adhesive; and III) Adper Easy Bond (3M ESPE), the mildest of the three self-etching adhesives. After the application of these adhesives to dentin according to the manufacturers' instructions, they were polymerized using a quartz-tungsten-halogen light-curing unit with an output intensity of 600 mW/cm^2. This was followed by incremental placement of two 2-mm thick layers of a resin composite that was light-cured separately for 40 sec each. The bonded teeth were stored at 100% relative humidity for 24 h. Each tooth was sectioned occluso-gingivally into 0.3-mm thick slabs, each containing the resin-dentin interface.

2.2 Remineralization medium

White Portland cement (Lehigh Cement Company, Allentown, Pennsylvania, USA) was mixed with deionized water in a water-to-powder ratio of 0.35:1, placed in flexible silicone molds and allowed to set and aged at 100% relative humidity for one week before use. A simulated body fluid (SBF) was prepared by dissolving 136.8 mM NaCl, 4.2 mM $NaHCO_3$, 3.0 mM KCl, 1.0 mM $K_2HPO_4{\cdot}3H_2O$, 1.5 mM $MgCl_2{\cdot}6H_2O$, 2.5 mM $CaCl_2$ and 0.5 mM Na_2SO_4 in deionized water and adding 3.08 mM sodium azide to prevent bacterial growth. This SBF also served as the control remineralization medium which contained no biomimetic analog. For the biomimetic remineralization medium, 500 μg/mL of polyacrylic acid (Mw = 1,800; Sigma-Aldrich, St. Louis, Illinois, USA) and 200 μg/mL of polyvinylphosphonic acid (Mw = 24,000; Sigma-Aldrich), were added to the SBF as dual biomimetic analogs. All solutions were buffered to pH 7.4 with 0.1 M Tris Base or 0.1 M HCl.

2.3 Biomimetic remineralization

Each control and experimental specimen slab was placed over a set Portland cement block (*c*a. 1 g) inside a glass scintillation vial. The latter was filled with 15 mL of SBF containing the two biomimetic analogs. Each glass vial was capped to prevent evaporation of the solution and stored in an incubator at 37°C. The remineralization medium was changed every month,

with its pH (after inclusion of Portland cement blocks) monitored weekly so that it was above 9.25. This ensured that apatite was formed instead of octacalcium phosphate [26]. Experimental and control specimens were retrieved after 1–4 months (four slabs per month) for ultrastructural examination of the extent of remineralization. Baseline specimens were examined before immersion for examination of the interdiffusion zone and for the presence of water-rich, resin-sparse regions using a silver nitrate tracer protocol [27].

2.4 Transmission electron microscopy

Following retrieval, the control and experimental specimen slabs were fixed in Karnovsky's fixative, rinsed in cacodylate buffer, post-fixed in 1% osmium tetroxide. After fixation, each slab was rinsed three times with sodium cacodylate buffer. The slab was dehydrated in an ascending ethanol series (50–100%), immersed in propylene oxide as a transitional medium and embedded in epoxy resin [28]. For each monthly examination period, non-demineralized, 90 nm thick sections were prepared and examined without further staining using a JEM-1230 TEM (JEOL, Tokyo, Japan) at 110 kV.

3. Results

3.1. Baseline Specimens

Baseline specimens were prepared from adhesive-bonded dentin slices that had not been subjected to remineralization. The three self-etching adhesives possessed different aggressiveness (i.e. pHs), as revealed by the different thickness and demineralization characteristic within the interdiffusion zones (Fig. 1). Adper Prompt, the most aggressive adhesive, created a 5 μm thick completely-demineralized interdiffusion zone (Fig. 1A). Adper Scotchbond SE, the moderately aggressiveness adhesive, created a 2 μm thick interdiffusion zone with a partially-demineralized basal region and a fully-demineralized surface region (Fig 1C). Adper Easy Bond, the mildest of the three self-etching adhesives created a 0.5 μm thick interdiffusion zone (Fig 1E). The basal 0.3 μm of this interdiffusion zone was partially-demineralized. Although the surface 0.2 μm of the interdiffusion zone appeared completely-demineralized at this magnification, very fine remnant apatite crystallites could be identified at high magnifications (not shown). Application of a silver nitrate tracer solution to those interdiffusion zones revealed water-rich, resin-sparse regions that contained electron-dense silver deposits (Figs. 1B, 1D, 1F). Additional water channels extended from the surface of the interdiffusion zones into the adhesive layers (Figs. 1D, 1F). They represent water derived from the originally water-filled dentinal tubules of the dentin substrate that was evaporated by the heat generated during polymerization of the adhesives and were trapped within the adhesive layers. Identification of those water-rich regions explained why resin-infiltrated demineralized collagen matrices are remineralizable after they have been filled with hydrophilic dental adhesive resins.

3.2. Control Specimens

Control specimens were prepared from bonded dentin slices after they had been immersed for 4 months in the control simulated body fluid medium. The completely-demineralized interdiffusion zone in Adper Prompt did not remineralize in the absence of biomimetic analogs [22]. For Adper Scotchbond SE and Adper Easy Bond, the thickness and density of the partially-demineralized regions within the interdiffusion zones increased after remineralization (Figs. 3A, 3B, 4A, 4B). Similar to Adper Prompt, the fully-demineralized, superficial part of the interdiffusion zone created by Adper Scotchbond SE did not remineralize in the absence of biomimetic analogs due to the depletion of remnant extrafibrillar and intrafibrillar seed crystallites (Figs. 3A, 3B). For Adper Easy Bond, the mildest adhesive, extrafibrillar remineralization along the periphery of the tufted collagen fibrils could be seen along the surface of the interdiffusion zone (Fig. 4B).

3.3. Experimental Specimens

Experimental specimens were prepared from bonded dentin slices that had been immersed in the biomimetic remineralization medium for 1–4 months. An early stage of remineralization that was seen in Adper Prompt is depicted in Fig. 2A. Remineralization occurred along the base of the originally completely-demineralized interdiffusion zone. As the spaces between the collagen fibrils were occupied by resin, remineralization was predominantly identified within the fibrils (i.e. intrafibrillar remineralization). In this “inchoate state”, remineralization appeared as continuous, braided electron-dense extensions that followed the microfibrillar arrangement of collagen fibrils (Fig. 2B). Figure 2C showed a more mature stage of remineralization in Adper Prompt in which the entire interdiffusion zone was remineralized. Transformation of the continuous, braided mineral phase into discrete intrafibrillar platelets could be seen within a single collagen fibril (Figs. 2D–2F).

For Adper Scotchbond SE, the fully-demineralized surface part of the interdiffusion zone was remineralized at an early stage (Fig. 3C). The mode of remineralization was intrafibrillar in nature and consisted of the electron-dense braided mineral phase (Fig. 3C). In some collagen fibrils, the continuity of the electron-dense mineral phase was interrupted by the appearance of short, non-overlapping mineral platelets that still retained the rope-like microfibrillar architecture [29] of the collagen fibrils (Fig. 3D). Unlike the baseline and control specimens (Figs. 1C, 3A), the entire interdiffusion zone was found to be occupied by minerals in experiment specimens with a more advanced stage of remineralization (Fig. 3E). Although remnant fibrils with the electron-dense braided mineral phase could still be seen, the surface part of the interdiffusion zone was predominantly filled with platelet-shaped minerals at this stage of remineralization (Fig. 3F).

For Adper Easy Bond, difference between the control and experimental specimens was most notable during the early stage of biomimetic remineralization. The extrafibrillar remineralization that was observed on the tufted fibrils along the surface of the interdiffusion zone in the control specimens (Fig. 4B) was replaced by intrafibrillar remineralization of similar tufted fibrils in the experimental specimens (Fig. 4C). In those experimental specimens, the characteristic electron-dense braided mineral phase could be seen within the fibrils, with occasional appearance of amorphous, electron-dense globular bodies adjacent to the braided fibrils (Fig. 4D). With a more mature stage of biomimetic remineralization, the braided fibrils were transformed into a denser conglomerate of mineral platelets that could be more easily identified along the surface tufted collagen fibrils (Fig. 4E). A high magnification view of the subsurface of the remineralized interdiffusion zone revealed collagen fibrils packed with mineral platelets that were much smaller than the adjacent platelets derived from the original partially-demineralized dentin (Fig. 4F). These miniature mineral platelets probably represent an intermediate stage of transformation of the “inchoate” braided mineral phase to the final “mature” platelet phase.

4. Discussion

The results obtained from the control specimens confirmed that remineralization of completely-demineralized dentin does not occur when biomimetic analogs are absent from a remineralization medium. Conversely, the increase in thickness and density of the partially-demineralized regions in control specimens prepared with Adper Scotchbond SE and Adper Easy Bond (Figs. 3A, 3B, 4A, 4B) indirectly indicated that remineralization of partially-demineralized dentin can occur in the absence of biomimetic analogs. This is probably due to the epitaxial growth over remnant seed crystallites which act as templates for mineral deposition [30], with the orientation of newly formed mineral lattice determined by the lattice of the underlying crystal. This process is quite common in the formation of calculus [31] and remineralization of enamel [32,33]. Such a top-down mechanism of crystal growth is probably

thermodynamically more favorable based on the classical crystallization theory. Crystallization proceeds via the one-step route of simply overcoming the free energy required for crystal growth (ΔG_{growth}), without the need to overcome simultaneously the activation-energy barrier for nucleation ($\Delta G_{nucleation}$). Thus, remineralization occurs without the need for the alternative kinetically-driven protein/polymer-modulated pathway for lowering the Gibbs free energy via sequential steps of phase transformations, as depicted by the nonclassical crystallization theory [15,34]. Although noncollagenous proteins may be associated with the remaining minerals in partially-demineralized dentin [35], we did not observe additional intrafibrillar remineralization of the completely-demineralized regions of the interdiffusion zones created by these two adhesives, contrary to the results suggested by Saito *et al*. [36]. However, it is possible that some of these noncollagenous proteins may participate in the top-down remineralization process by inhibiting the dimensions of the apatite crystallites during the process of epitaxial growth [37].

In this study, we could only speculate the occurrence of epitaxial crystal growth based on the increase in thickness and density of the partially-demineralized regions of the interdiffusion zones. This is due to our inability to distinguish newly precipitated mineral phase from the existing mineral core with the use of conventional TEM. Direct evidence of epitaxial crystal growth requires the use of high resolution-TEM (HR-TEM) that permits examining the orientation of lattice fringes in those crystals and to identify possible interfacial dislocations and lattice mismatch between the precipitating phase and the existing crystal core [38,39]. Another method which we have recently adopted in our laboratory is to induce heteroepitaxial growth on apatite seed crystallites. This may be achieved by or substituting the calcium ions in the apatite hexagonal $P6_3/m$ lattice with lead or strontium [40,41], the phosphate ions with vanadate [42] by incorporating inorganic salts containing these replacement ions in the remineralization media. This will enable us to detect evidence of epitaxial growth derived from a top-down remineralization approach using energy dispersive X-ray microanalysis in conjunction with a conventional TEM.

The aforementioned top-down remineralization mechanism is applicable only, on a nanoscopical scale, to those parts of a collagen fibril that contain seed crystallites. This is exemplified by the high magnification TEM image in Fig. 4B. Extrafibrillar crystallites were attached only to the some parts of the collagen fibril surface, while other locations along the same fibril were completely devoid of extrafibrillar mineral platelets. This mode of remineralization differed drastically from results achieved with the bottom-up approach when the dual biomimetic analogs were included in the remineralization medium. Intrafibrillar remineralization in the form of the electron-dense braided mineral phase was the first sign of bottom-up remineralization to be appeared in the apatite-depleted regions of all three adhesives. This “inchoate” state of mineralization, depicted at high magnification in Fig. 4D, has the unique characteristic of recapitulating the microfibrillar subunits of a collagen fibril [43,44] and is schematically represented by Fig. A of Scheme 1. Similar features were also observed in the recent study by Deshpande and Beniash [45] after non-resin-infiltrated, reconstituted, single collagen fibrils were remineralized in the presence of poly(L-aspartic acid). Although the nature of the two studies was different, important conclusions may be drawn when the findings from the elegant work by Deshpande and Beniash were compared with our present results.

In the Deshpande and Beniash study, the authors reported using selected area electron diffraction that the minerals that were formed within two hours were initially amorphous. The amorphous nature of this mineral phase gradually decreased and became exclusively crystalline after 16 hours. In the present study, the initially continuous nature of the braided mineral phase became discrete nanocrystals that still captured the microfibrillar arrangement of the collagen fibrils. We interpreted these findings as complementary manifestations of the same

phenomenon. The only difference is that in the Deshpande and Beniash study, the authors examined whole remineralized collagen fibrils without sectioning; in the present study, sections through the remineralized fibrils were examined, thereby enabling a clearer depiction of the internal structure of the transformed crystalline phase. Although we had performed selected area electron diffraction on these remineralized phases (not shown), our distinction between the amorphous and crystalline nature of these mineral phases was less clear cut due to the three dimensional, closely approximated nature of a natural collagen matrix. In the Deshpande and Beniash study, the collagen fibrils were in direct contact with the poly(aspartic acid)-containing solution. Thus, amorphous calcium phosphate (ACP) nanoprecursor phases required minimal diffusion distances to reach the collagen fibrils. In the present study, the collagen matrices were encapsulated by hydrophilic adhesive resins. Although the latter permits the ingress of water via diffusion channels (Figs. 1B, 1D, 1F), they were considerably more tortuous. The water-rich, resin-sparse channels between the collagen fibrils were also occupied by water-sorbed, space-filling glycosaminoglycans [46] that could have prolonged the time required for the fluidic ACP nanoprecursors to reach the collagen fibrils. Collectively, these issues account for the longer time required for the remineralization of resin-bonded dentin (months) when compared to the much shorter time (hours) required for the remineralization of a single layer of widely separated, reconstituted collagen fibrils that were prepared from purified, glycosaminoglycans-depleted collagen solutions.

The fact that these nanoprecursors can penetrate the hydrophilic resin polymer matrix that occupied the extrafibrillar spaces around the collagen fibrils was indicative of the fluidic nature of these nanoprecursors. The liquid-like ACP nanoprecursors described above has been referred by Gower and her colleagues [16,47] as polymer induced liquid precursors, based on their initial work on polyanionic acid stabilized amorphous calcium carbonate phases. Similar to poly(aspartic acid), polyacrylic acid, one of the two biomimetic analogs employed in the present study, has the ability to sequester the ACP phases into droplets that are smaller than the wavelength of light, so that they appeared transparent to the naked eye [48]. The layer of low molecular weight polyacrylic acid around the amorphous calcium phosphate probably functions as a surfactant [48], permitting liquid-liquid phase separation of the ACP nanoprecursors from the aqueous remineralization medium [16]. Penetration and coalescence of individual nanodroplets results in a continuous phase of amorphous calcium salts within the collagen fibril [16]. Examples of these amorphous fluid phases, approximately 50 nm in diameter, are illustrated in Figs. 2B and 4D. The amorphous structure depicted in Fig. 2B is particularly interesting as it presented with an appendage that appeared to be in contact with a collagen fibril that was infiltrated with the electron-dense continuous, braided mineral phase. These features are schematically represented in Figs. B of Scheme 1. Although observation of these amorphous structures in the present study may be incidental, we have been able to observe large quantities of larger amorphous, electron-dense droplets that congregated around the periphery of the collagen fibrils when much high concentrations of polyvinylphosphonic acid than the concentration employed in the present study were directly applied to acid-etched dentin prior to adhesive application (Supplemental Material – S1 and S2). Usually, these transient, metastable amorphous droplets are difficult to detect unless special techniques such as dynamic light scattering [49] or cryo-scanning electron microscopy [50] are employed. A possible reason why these droplets could be identified in our studies may be due to their entanglement within the polymer network of a resin matrix. This is similar to the results by Liou *et al.* when the polyacrylic acid stabilized apatitic nanospheres were dispersed within the polyacrylic acid matrix of a nanocomposite [48]. More recent studies suggested that these fluidic nanoprecursors may be the result of the aggregation of even smaller (0.6–1.1 nm) amorphous prenucleation ionic clusters [17,51]. Such works are based on the more thoroughly studied calcium carbonate systems and the existence of prenucleation calcium phosphate clusters has yet to be identified. Nevertheless, based on the nonclassical crystallization theory, both prenucleation clusters and polymer-stabilized amorphous nanoprecursors may be the first two

steps [17] in a kinetically-driven cascade targeted at minimizing the activation-energy barriers in a crystallization event [52].

The observation that intrafibrillar remineralization occurred in our present systems indicated that the internal environment of those remineralized fibrils were occupied by water instead of resin. Remineralization of the collagen fibrils would require that the free water within the collagen fibrils and loosely-bound water within the collagen molecules be replaced by liquid-like ACP nanoprecursors (Fig. C1 of Scheme 1). A recent magnetic response microscopy study showed that there was a reduction in the mobility of water molecules, as indicated by a reduction in the water proton transverse (T_2) relaxation times, as water in the collagen fibrils was replaced by amorphous calcium phosphate precursors [53]. Thus mineralization of collagen fibrils may be perceived as a dehydration process.

Template-directed transformation of the coalesced amorphous precursor phase into polycrystalline phases [17,18] could be identified along different parts of the same collagen fibrils in the present study (Figs. 2D, 2E). This is schematically represented by Figs. C2, D1 and D2 in Scheme 1. Polyvinylphosphonic acid (PVPA), the other analog present in the biomimetic remineralization medium, is a polyanion that mimics phosphoproteins such as DMP-1, phosphophoryn or bone sialoprotein [37]. Unlike phosphoprotein molecules that bind to specific sites along the collagen molecules, PVPA is conjectured to bind nonspecifically to the collagen molecules (*Gu et al., unpublished results*). Similar to natural phosphoproteins, they may act as templates that trigger transformation of the coalesced amorphous precursors into nanocrystalline domains inside the amorphous structures [54]. Stabilized by the templating molecules, these nanocrystalline domains undergo subsequent growth into oriented single crystals [17]. This protein/polymer-dependent bottom-up assembly of nanocrystalline domains into single crystals has been referred to as mesoscopic transformation [15,52]. In the present study, this sequence of events is exemplified by the conversion of the continuous braided mineral phase into discrete, nonoverlapping nanocrystals (Fig. 3D), and ultimately into larger overlapping platelets or needles (Figs. 2E, 2F), depending upon the plane of sectioning (Fig. D2 of Scheme 1).

It is not possible to provide direct evidence of mesoscopic transformation based on electron microscopy observations alone. However, indirect evidence may be obtained by comparing the configuration of the continuous braided mineral phase versus the post transformation overlapping platelet phase identified from the TEM images. The microfibril model proposed by Smith considered packing of a bundle of five intertwining triple helical collagen molecules into microfibrillar subunits within a collagen fibril [55,56]. According to Holmes *et al*. [57], a cross-section of 100 nm diameter collagen fibril would contain approximately 3900 collagen molecules. This is equivalent to 780 microfibrils in a 100 nm diameter collagen fibril. Indeed, a longitudinal section through a collagen fibril that was infiltrated the continuous braided mineral phase (Fig. 4D) appeared to support the presence of a large number of microfibrils within the collagen fibril. However, irrespective of the plane of sectioning (Figs. 3D,4F), the number of transformed nanocrystalline phases that were sequentially produced within a 100 nm diameter fibril was less than ten in number. These nanocrystalline phases, in turn, were much smaller in dimensions when compared to the more mature platelets observed in Figs. 2F and 4F. The only way to account for this reduction in the number of electron-dense strands to the number of platelets seen in the mature remineralized fibrils is the initial condensation of the amorphous mineral phase into metastable nanocrystalline phases, followed by their mesoscopic transformation into larger crystallites. These observations appear to support the cascade of events proposed by the mechanism of bottom-up, template-directed, particle-based assembly of metastable nanocomponents into single crystalline structures [17,18]. A hypothetical depiction of this transition from nanocrystalline phase into larger crystalline platelets is depicted in Fig. E of Scheme 1.

4. Conclusion

Biomimetic remineralization research has advanced considerably over the last decade. From earlier studies that demonstrated predominantly extrafibrillar remineralization [58,59] to the more recent studies that verified that reconstituted collagen scaffolds or individual fibrils [45,47] are capable of intrafibrillar remineralization, the progress has been nothing short of phenomenal. The discovery of a cascade of metastable phases such as liquid-like amorphous precursors and mesocrystals has further advanced our knowledge on how biomineralization may be biomimetically recapitulated based on the non-classical theory of crystallization.

Calcium and phosphate releasing materials have been available for almost three decades for remineralizing the apatite minerals lost due to the carious process. The majority of these studies were based on the deposition of newly formed calcium phosphate phases over remnant seed crystallites, in compliance with the principles of the classical theory of crystallization. The question exists whether existing systems can remineralize those parts of a collagen matrix that are devoid of seed crystallites. In this study, it was found that in the absence biomimetic analogs in a remineralization medium, remineralization only occurred in partially-demineralized collagen matrices probably by epitaxial growth. Conversely, in the presence of biomimetic analogs in the remineralization medium, intrafibrillar remineralization of completely-demineralized collagen matrices can additionally be identified. The success of the current proof-of-concept, laterally-diffusing remineralization protocol warrants the development of a clinically-applicable delivery system by incorporating these biomimetic analogs into the steps involved in the application of these adhesives and filling materials.

Supplementary Material

Refer to Web version on PubMed Central for supplementary material.

Acknowledgments

This study was supported by Grant R21 DE019213-01 from the National Institute of Dental and Craniofacial Research (PI. Franklin R. Tay). We thank Thomas Bryan for epoxy resin embedding, Robert Smith for TEM support and Michelle Barnes for secretarial support.

References

1. Featherstone JD. The science and practice of caries prevention. J Am Dent Assoc 2000;131:887–99. [PubMed: 10916327]
2. Linde A. Dentin matrix proteins: composition and possible functions in calcification. Anat Rec 1989;224:154–66. [PubMed: 2672882]
3. Goldberg M, Takagi M. Dentine proteoglycans: composition, ultrastructure and functions. Histochem J 1993;25:781–806. [PubMed: 7507908]
4. Hebling J, Pashley DH, Tjäderhane L, Tay FR. Chlorhexidine arrests subclinical degradation of dentin hybrid layers in vivo. J Dent Res 2005;84:741–6. [PubMed: 16040733]
5. Carrilho MR, Geraldeli S, Tay FR, de Goes MF, Carvalho RM, Tjäderhane L, Reis AF, Hebling J, Mazzoni A, Breschi L, Pashley DH. In vivo preservation of the hybrid layer by chlorhexidine. J Dent Res 2007;86:529–33. [PubMed: 17525352]
6. Brackett WW, Tay FR, Brackett MG, Dib AR, Sword J, Pashley DH. The effect of chlorhexidine on dentin hybrid layers in vivo. Oper Dent 2007;32:107–11. [PubMed: 17427817]
7. Pashley DH, Tay FR, Yiu C, Hashimoto M, Breschi L, Carvalho RM, Ito S. Collagen degradation by host-derived enzymes during aging. J Dent Res 2004;83:216–21. [PubMed: 14981122]
8. Trebacz H, Wójtowicz K. Thermal stabilization of collagen molecules in bone tissue. Int J Biol Macromol 2005;37:257–62. [PubMed: 16414113]

9. Honda Y, Kamakura S, Sasaki K, Suzuki O. Formation of bone-like apatite enhanced by hydrolysis of octacalcium phosphate crystals deposited in collagen matrix. J Biomed Mater Res B Appl Biomater 2007;80:281–9. [PubMed: 16850470]
10. Boskey AL. Biomineralization: an overview. Connect Tissue Res 2003;44(Suppl 1):5–9. [PubMed: 12952166]
11. Goldberg HA, Warner KJ, Li MC, Hunter GK. Binding of bone sialoprotein, osteopontin and synthetic polypeptides to hydroxyapatite. Connect Tissue Res 2001;42:25–37. [PubMed: 11696986]
12. Zhang S. Fabrication of novel biomaterials through molecular self-assembly. Nat Biotechnol 2003;21:1171–8. [PubMed: 14520402]
13. Tay FR, Pashley DH. Guided tissue remineralisation of partially demineralised human dentine. Biomaterials 2008;29:1127–37. [PubMed: 18022228]
14. Gajjeraman S, Narayanan K, Hao J, Qin C, George A. Matrix macromolecules in hard tissues control the nucleation and hierarchical assembly of hydroxyapatite. J Biol Chem 2007;282:1193–1204. [PubMed: 17052984]
15. Xu A, Ma Y, Cölfen H. Biomimetic mineralization. J Mater Chem 2007;17:415–49.
16. Gower LB. Biomimetic model systems for investigating the amorphous precursor pathway and its role in biomineralization. Chem Rev 2008;108:4551–627. [PubMed: 19006398]
17. Pouget EM, Bomans PH, Goos JA, Frederik PM, de With G, Sommerdijk NA. The initial stages of template-controlled CaCO3 formation revealed by cryo-TEM. Science 2009;323:1455–8. [PubMed: 19286549]
18. Tsuji T, Onuma K, Yamamoto A, Iijima M, Shiba K. Direct transformation from amorphous to crystalline calcium phosphate facilitated by motif-programmed artificial proteins. Proc Natl Acad Sci USA 2008;105:16866–70. [PubMed: 18957547]
19. Yu S. Bio-inspired Crystal Growth by Synthetic Templates. Top Curr Chem 2007;271:79–118.
20. Wong TS, Brough B, Ho CM. Creation of functional micro/nano systems through top-down and bottom-up approaches. Mol Cell Biomech 2009;6:1–55. [PubMed: 19382535]
21. Tay FR, Pashley DH. Biomimetic remineralization of resin-bonded acid-etched dentin. J Dent Res 2009;88:719–24. [PubMed: 19734458]
22. Mai S, Kim YK, Toledano M, Breschi L, Ling JQ, Pashley DH, Tay FR. Phosphoric acid esters cannot replace polyvinylphosphonic acid as phosphoprotein analogs in biomimetic remineralization of resin-bonded dentin. Dent Mater 2009;25:1230–9. [PubMed: 19481792]
23. Doi Y, Eanes ED. Transmission electron microscopic study of calcium phosphate formation in supersaturated solutions seeded with apatite. Calcif Tissue Int 1984;36:39–47. [PubMed: 6423234]
24. Bertassoni LE, Habelitz S, Kinney JH, Marshall SJ, Marshall GW Jr. Biomechanical perspective on the remineralization of dentin. Caries Res 2009;43:70–7. [PubMed: 19208991]
25. Tay FR, Pashley DH. Aggressiveness of contemporary self-etching systems. I: Depth of penetration beyond dentin smear layers. Dent Mater 2001;17:296–308. [PubMed: 11356206]
26. Meyer JL, Eanes ED. A thermodynamic analysis of the secondary transition in the spontaneous precipitation of calcium phosphate. Calcif Tissue Res 1978;25:209–16. [PubMed: 30523]
27. Tay FR, Pashley DH, Yoshiyama M. Two modes of nanoleakage expression in single-step adhesives. J Dent Res 2002;81:472–6. [PubMed: 12161459]
28. Tay FR, Moulding KM, Pashley DH. Distribution of nanofillers from a simplified-step adhesive in acid-conditioned dentin. J Adhes Dent 1999;1:103–17. [PubMed: 11725676]
29. Bozec L, van der Heijden G, Horton M. Collagen fibrils: nanoscale ropes. Biophys J 2007;92:70–5. [PubMed: 17028135]
30. Donnet M, Bowen P, Jongen N, Lemaître J, Hofmann H. Use of seeds to control precipitation of calcium carbonate and determination of seed nature. Langmuir 2005;21:100–8. [PubMed: 15620290]
31. Rohanizadeh R, Legeros RZ. Ultrastructural study of calculus-enamel and calculus-root interfaces. Arch Oral Biol 2005;50:89–96. [PubMed: 15598421]
32. Iijima M, Tohda H, Suzuki H, Yangisawa T, Moriwaki Y. Effects of F^{-} on apatite-octacalcium phosphate intergrowth and crystal morphology in a model system of tooth enamel formation. Cal Tissue Int 1992;50:357–61.

33. Fan Y, Sun Z, Moradian-Oldak J. Controlled remineralization of enamel in the presence of amelogenin and fluoride. Biomaterials 2009;30:478–83. [PubMed: 18996587]
34. Wang L, Nancollas GH. Pathways to biomineralization and biodemineralization of calcium phosphates: the thermodynamic and kinetic cont rols. Dalton Trans 2009;15:2665–72. [PubMed: 19333487]
35. Clarkson BH, Feagin FF, McCurdy SP, Sheetz JH, Speirs R. Effects of phosphoprotein moieties on the remineralization of human root caries. Caries Res 1991;25:166–73. [PubMed: 1652358]
36. Saito T, Yamauchi M, Crenshaw MA. Apatite induction by insoluble dentin collagen. J Bone Miner Res 1998;13:265–70. [PubMed: 9495520]
37. George A, Veis A. Phosphorylated proteins and control over apatite nucleation, crystal growth, and inhibition. Chem Rev 2008;108:4670–93. [PubMed: 18831570]
38. Aoba T, Yoshioka C, Yagi T, Moreno EC. High-resolution electron microscopy of hydroxyapatite grown in dilute solutions. J Dent Res 1984;63:1348–54. [PubMed: 6096429]
39. Nelson DG, Barry JC. High resolution electron microscopy of nonstoichiometric apatite crystals. Anat Rec 1989;224:265–76. [PubMed: 2672890]
40. Ellis DE, Terra J, Warschkow O, Jiang M, González GB, Okasinski JS, Bedzyk MJ, Rossi AM, Eon J-G. A theoretical and experimental study of lead substitution in calcium hydroxyapatite. Phys Chem Chem Phys 2006;8:967–76. [PubMed: 16482339]
41. O'Donnell MD, Fredholm Y, de Rouffignac A, Hill RG. Structural analysis of a series of strontium-substituted apatites. Acta Biomater 2008;4:1455–64. [PubMed: 18502710]
42. Pizzala H, Caldarelli S, Eon JG, Rossi AM, Laurencin D, Smith ME. A solid-state NMR study of lead and vanadium substitution into hydroxyapatite. J Am Chem Soc 2009;131:5145–52. [PubMed: 19317471]
43. Trus BL, Piez KA. Compressed microfibril models of the native collagen fibril. Nature 1980;286:300–1. [PubMed: 7402317]
44. Castellani PP, Morocutti M, Franchi M, Ruggeri A, Bigi A, Roveri N. Arrangement of microfibrils in collagen fibrils of tendons in the rat tail. Ultrastructural and x-ray diffraction investigation. Cell Tissue Res 1983;234:735–43. [PubMed: 6661761]
45. Deshpande AS, Beniash E. Bioinspired Synthesis of Mineralized Collagen Fibrils. Crystal Growth & Design 2008;8:3084–90. [PubMed: 19662103]
46. Mazzoni A, Pashley DH, Ruggeri A Jr, Vita F, Falconi M, Di Lenarda R, Breschi L. Adhesion to chondroitinase ABC treated dentin. J Biomed Mater Res B Appl Biomater 2008;86:228–36. [PubMed: 18161809]
47. Olszta MJ, et al. Bone structure and formation: A new perspective. Mat Sc Eng R 2007;58:77–116.
48. Liou SC, Chen SY, Liu DM. Manipulation of nanoneedle and nanosphere apatite/poly(acrylic acid) nanocomposites. J Biomed Mater Res B Appl Biomater 2005;73:117–22. [PubMed: 15672405]
49. DiMasi E, Liu T, Olszta MJ, Gower LB. Laser Light Scattering Observations of Liquid-Liquid Phase Separation in a Polymer-Induced Liquid-Precursor (PILP) Mineralization Process. Mater Res Soc Symp Proc 2005;873E:K10.6.
50. Wolf SE, Leiterer J, Kappl M, Emmerling F, Tremel W. Early homogenous amorphous precursor stages of calcium carbonate and subsequent crystal growth in levitated droplets. J Am Chem Soc 2008;130:12342–7. [PubMed: 18717561]
51. Gebauer D, Völkel A, Cölfen H. Stable prenucleation calcium carbonate clusters. Science 2008;322:1819–22. [PubMed: 19095936]
52. Cölfen H, Mann S. Higher-Order Organization by Mesoscale Self-Assembly and Transformation of Hybrid Nanostructures. Angew Chem Int Ed 2003;42:2350–65.
53. Chesnick IE, Mason JT, Giuseppetti AA, Eidelman N, Potter K. Magnetic resonance microscopy of collagen mineralization. Biophys J 2008;95:2017–26. [PubMed: 18487295]
54. Zhang TH, Liu XY. How Does a transient amorphous precursor template crystallization. J Am Chem Soc 2007;129:13520–6. [PubMed: 17929918]
55. Smith JW. Molecular pattern in native collagen. Nature 1968;219:157–8. [PubMed: 4173353]
56. King G, Brown EM, Chen JM. Computer model of a bovine type I collagen microfibril. Protein Eng 1996;9:43–9. [PubMed: 9053901]

57. Holmes DF, Graham HK, Trotter JA, Kadler KE. STEM/TEM studies of collagen fibril assembly. Micron 2001;32:273–85. [PubMed: 11006507]

58. Bradt J-H, Mertig M, Teresiak A, Pompe W. Biomimetic mineralization of collagen by combined fibril assembly and calcium phosphate formation. Chem Mater 1999;11:2694–701.

59. Zhang W, Liao SS, Cui FZ. Hierarchical self-assembly of nanofibrils in mineralized collagen. Chem Mater 2003;15:3221–6.

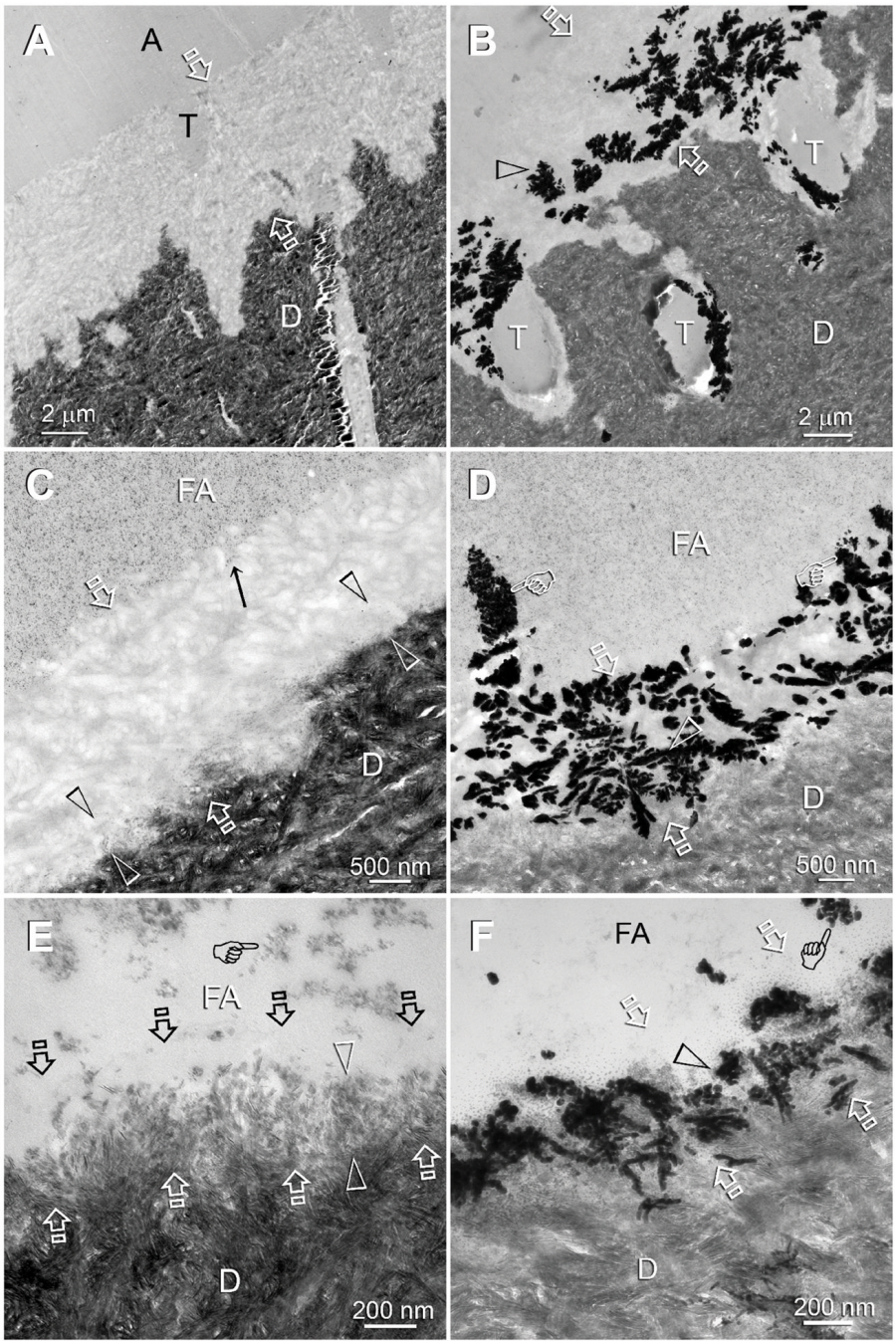

Figure 1.

TEM images of specimens that had not been subjected to biomimetic remineralization. These images provided baseline information on the depth of demineralization and extent of apatite dissolution in human dentin bonded with the three self-etch adhesives. Generic abbreviations - A: unfilled adhesive; FA: filled adhesive; D: dentin; T: dentinal tubule; Between open arrows: zone of demineralized dentin that was simultaneously infiltrated by the self-etch adhesive to produce an interdiffusion zone. **A**. Adper Prompt, the most aggressive adhesive, created a 5 **Δ**m thick layer of completely-emineralized dentin. **B**. Adper Prompt-bonded dentin that had been immersed in a silver nitrate tracer solution. The electron dense silver deposits (open arrowhead) revealed water-rich, resin-sparse regions within the interdiffusion zone. **C**. Adper

Scotchbond SE, a moderately aggressiveness adhesive, created a 2 **Λ**m thick interdiffusion zone. A thin, partially-demineralized region (between open arrowheads) could be identified along the base of the interdiffusion zone. **D**. The corresponding silver impregnated section of Adper Scotchbond SE showing water-rich, resin-sparse regions (open arrowhead) within the interdiffusion zone. Some of the water channels (pointers) extended vertically from the dentin surface into the filled adhesive. **E**. Adper Easy Bond, the mildest of the three self-etch adhesives, created a 500 nm thick interdiffusion zone with a clearly discernible 300 nm thick partially-demineralized region along its base (between open arrowheads). Although the surface 200 nm part of the interdiffusion zone appeared completely-demineralized at this magnification, very fine remnant apatites could be identified at higher magnification. **F**. The corresponding silver impregnated section of Adper Easy Bond showing water channels (open arrowhead) within the interdiffusion zone and in the filled adhesive (pointer).

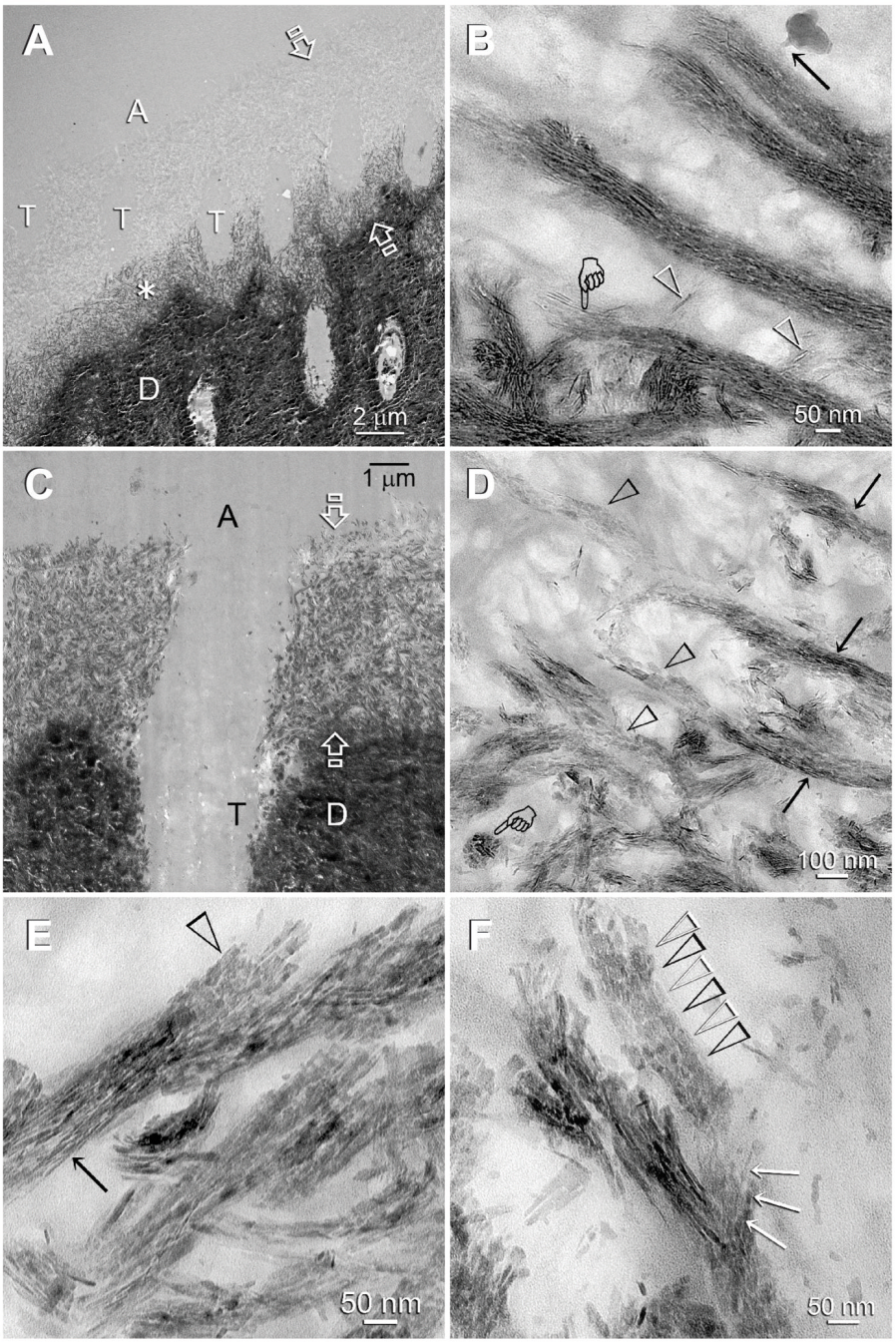

Figure 2.

TEM images of experimental Adper Prompt specimens that had undergone biomimetic remineralization. The completely-demineralized resin infiltrated collagen matrices of the control specimens did not remineralize in the absence of biomimetic analogs (not shown). A: adhesive; D: dentin; T: dentinal tubule. **A**. A representative example of a specimen that exhibited features of an early stage of biomimetic remineralization. Partial remineralization (asterisk) occurred along the base of the original zone of completely-demineralized dentin (between open arrows). **B**. A high magnification view of Fig. 2A. Intrafibrillar remineralization could be seen in the form of an electron-dense, continuous ribbon-like mineral phase (pointer) that extended along the longitudinal axis of the collagen fibrils, accentuating the braided

microfibrillar architecture of those remineralized fibrils. An electron-dense, amorphous droplet-like structure could be seen with an appendage extending into a remineralized collagen fibril (arrow). Individual intrafibrillar mineral platelets could not be identified at this stage. Extrafibrillar remineralization was minimal as the spaces between the collagen fibrils were filled with adhesive resins, and appeared in the form of needle-shaped crystallites (open arrowheads). **C.** A representative example of a specimen that exhibited features of a more mature stage of biomimetic remineralization. Intrafibrillar remineralization could be seen almost within the entire width of the original demineralized collagen matrix (between open arrows). **D.** A moderately high magnification view of Fig. 2C showing transformation of the continuous braided mineral phase (arrows) into discrete platelets (open arrowheads) within the same collagen fibrils. A transverse section through a remineralized fibril (pointer) clearly showed that it was fully filled with intrafibrillar minerals. **E**. A high magnification view, taken from a different specimen, illustrating the transition of the continuous braided mineral phase (arrow) into discrete platelets (open arrowhead) within a remineralized collagen fibril. This is the first time such a transformation has ever been demonstrated in situ within the same fibril (*see also* Fig. 3D). **F**. In this high magnification view, the remineralized fibril at the bottom still retained some of the continuous braided mineral phase (arrows), while the mineral phase within the fibril at the top had been transformed completely into discrete platelets (open arrowheads).

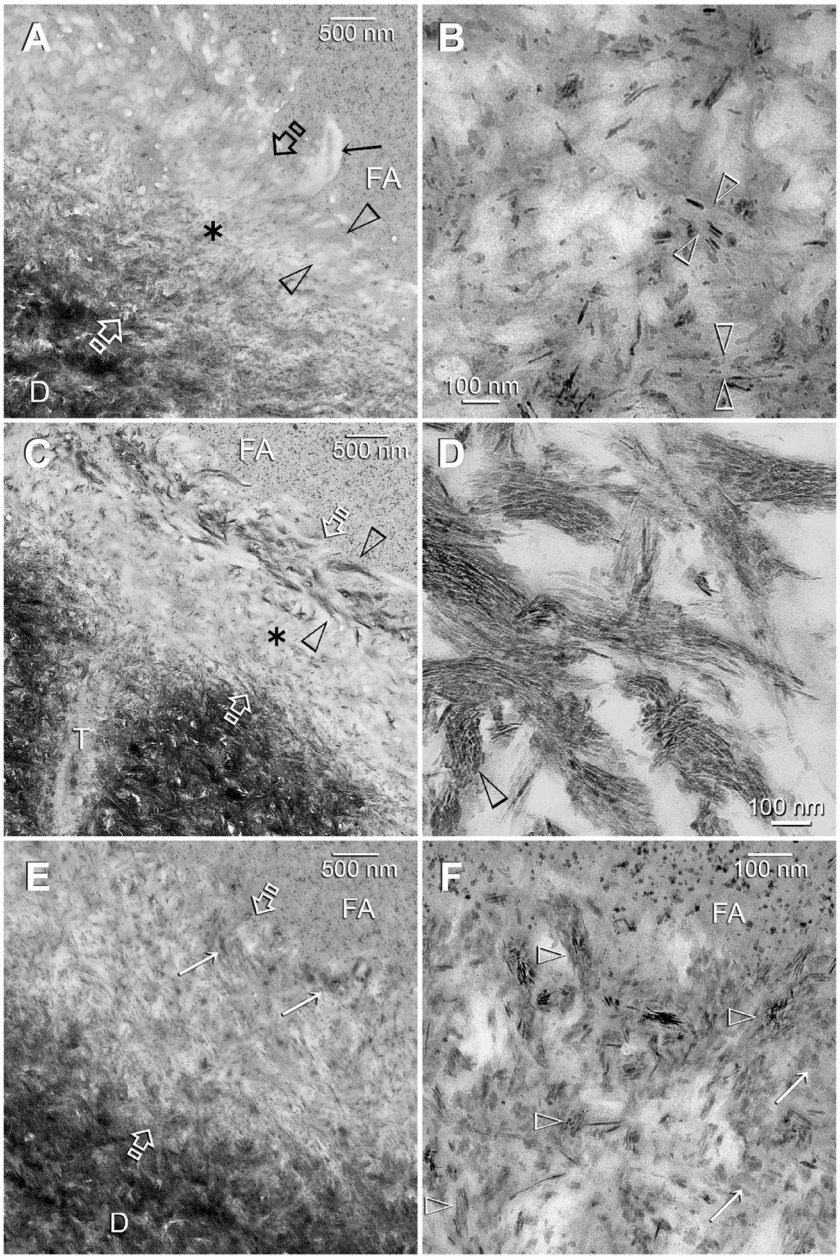

Figure 3.

TEM images of control (A–B) and experimental (C–F) dentin specimens bonded with Adper Scotchbond SE. FA: filled adhesive; D: dentin; T: dentinal tubule; Between open arrows: the original 2**Λ**m thick, partially demineralized interdiffusion zone. **A**. A control specimen that was retrieved after immersion in the Ca^{2+} and PO_4^{3-}-containing simulated body fluid (SBF) for the entire experimental period. There was an increase in the thickness and density of the partially-demineralized region within the interdiffusion zone, probably due to epitaxial growth over remnant seed crystallites (*see* Fig. 1C). However, in the absence of biomimetic analogs, there was no remineralization of the surface, completely-demineralized part of the interdiffusion zone (between open arrowheads). The surface collagen fibrils (arrow) were electron lucent (i.e. devoid of minerals). **B**. A high magnification view of the location marked by the asterisk in Fig. 3A. Remineralization was predominantly extrafibrillar along the surface

of the collagen fibrils (between open arrowheads). Intrafibrillar remineralization could not be recognized, probably due to depletion of remnant intrafibrillar seed crystallites from this location. **C**. An experimental specimen that exhibited features of an early stage of biomimetic remineralization. Unlike the control specimen (Fig. 3A), the surface part of the interdiffusion zone (between open arrowheads) was remineralized when biomimetic analogs are included in the SBF. The mode of remineralization was intrafibrillar in nature and consisted of the electron dense braided mineral phase that at this stage appeared completely different from the mineral phase present in the underlying interdiffusion zone (asterisk). **D**. A high magnification view of the electron dense braided mineral phase in Fig. 3C. In some collagen fibrils, the continuous electron dense phase had been transformed into discrete nanocrystals that followed the braided appearance of the microfibrillar strands (open arrowhead). **E**. An experimental specimen that exhibited features of a more mature stage of biomimetic remineralization. Minerals were present within the entire interdiffusion zone. Remnant braided mineral phases (arrows) could still be identified along the superficial part of the interdiffusion zone. **F**. A high magnification view of the superficial part of the interdiffusion zone showing the presence of mineral platelets (arrows) within a region that was completely-demineralized in the baseline (Fig. 1C) and control specimens (Fig. 3A). Remnants of the nanocrystals (open arrowheads) could be identified within this region.

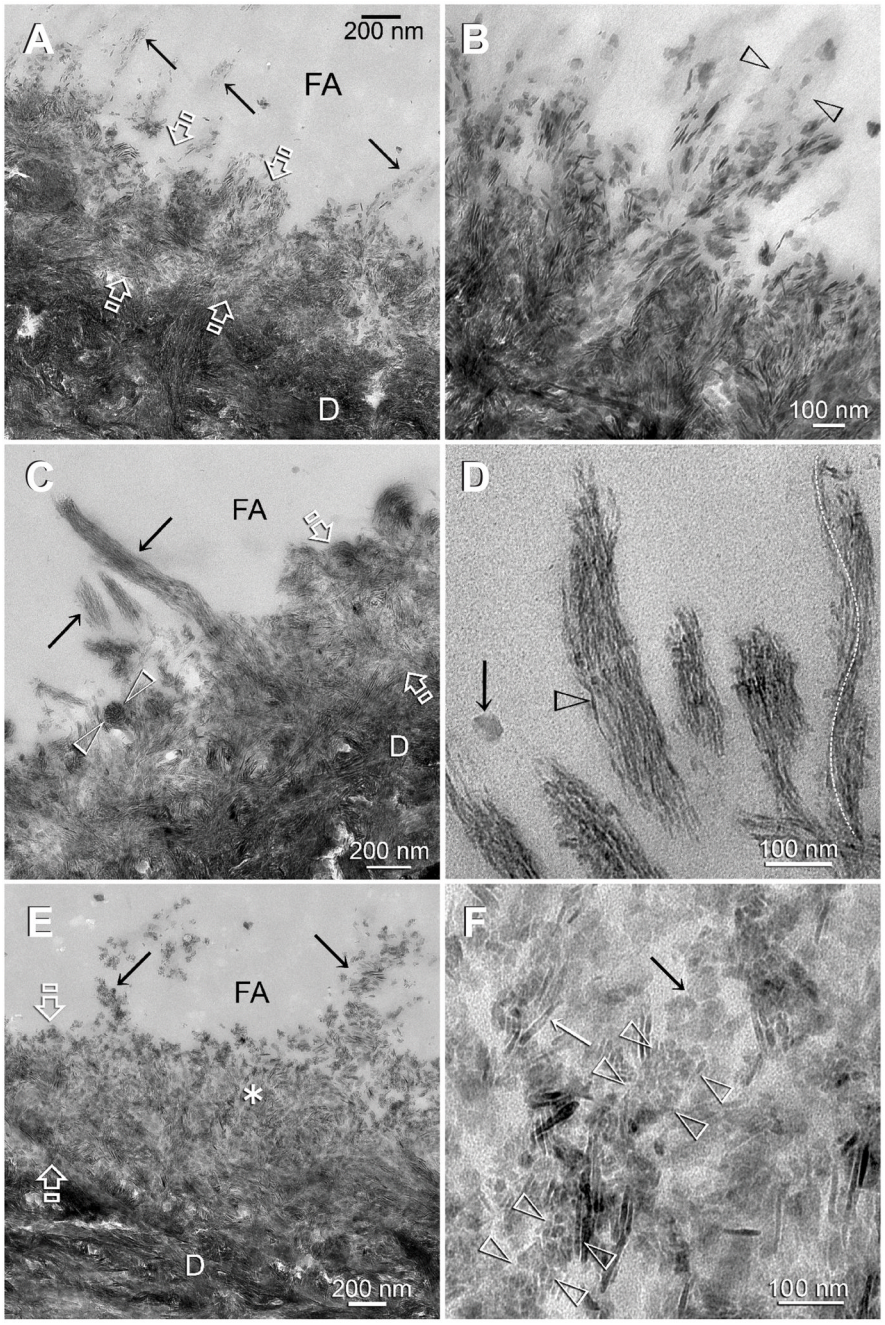

Figure 4.

TEM images of control (A–B) and experimental (C–F) dentin specimens bonded with Adper Easy Bond. FA: filled adhesive; D: dentin; T: dentinal tubule; Between open arrows: the original 0.5 **Δ**m thick, partially demineralized interdiffusion zone. **A**. In the absence of biomimetic analogs, remineralization of the interdiffusion zone probably occurred via epitaxial growth over remnant intrafibrillar and extrafibrillar seed crystallites. Some of the tufted collagen fibrils along the surface of the interdiffusion zone (arrows) also appeared to have remineralized. **B**. A high magnification view of those surface collagen fibrils in the control specimen showing that remineralization was extrafibrillar in nature, along the some parts surface of the collagen fibril (between open arrowheads), while other parts of the same fibril

were not remineralized. **C**. An experimental specimen that exhibited features of an early stage of biomimetic remineralization. Collagen fibrils within the entire interdiffusion zone contained the electron dense braided mineral phase, masking the existing apatite platelets from the original partially demineralized part of the interdiffusion zone. The electron-dense braided mineral phase was more easily observed from the tufted surface collagen fibrils (arrows). A collagen fibril that was sectioned transversely (between open arrowheads) clearly indicated that the entire fibril was filled with intrafibrillar minerals. **D**. A high magnification view of the remineralized, tufted collagen fibrils similar to those shown in Fig. 4C indicated that the electron-dense braided mineral phase remained continuous at this stage (open arrowhead). This electron-dense mineral phase followed the helical arrangement of the microfibrils (white dotted line). The electron-dense, amorphous structure (arrow) adjacent to the remineralized fibrils could represent a fluidic amorphous calcium phosphate nanoprecursor droplet (*see* Fig. 2B). **E**. An experimental specimen that exhibited features of a more mature stage of biomimetic remineralization. At this magnification, the bulk of the interdiffusion zone and the tufted surface collagen fibrils (arrows) were filled with mineral platelets. The electron-dense braided mineral phase could no longer be observed. **F**. A high magnification view taken from the location marked by the asterisk in Fig. 4E. Interpretation of the micrograph was complicated by the superimposition of remineralized minerals over existing minerals. A longitudinal section through a collagen fibril (between arrowheads) showed that it was filled with miniature mineral platelets that were much smaller than some of the adjacent platelets (arrows). Those miniature mineral platelets probably represented the transformed platelet phase from the continuous electron-dense braided mineral phase (*see* Fig. 3D).

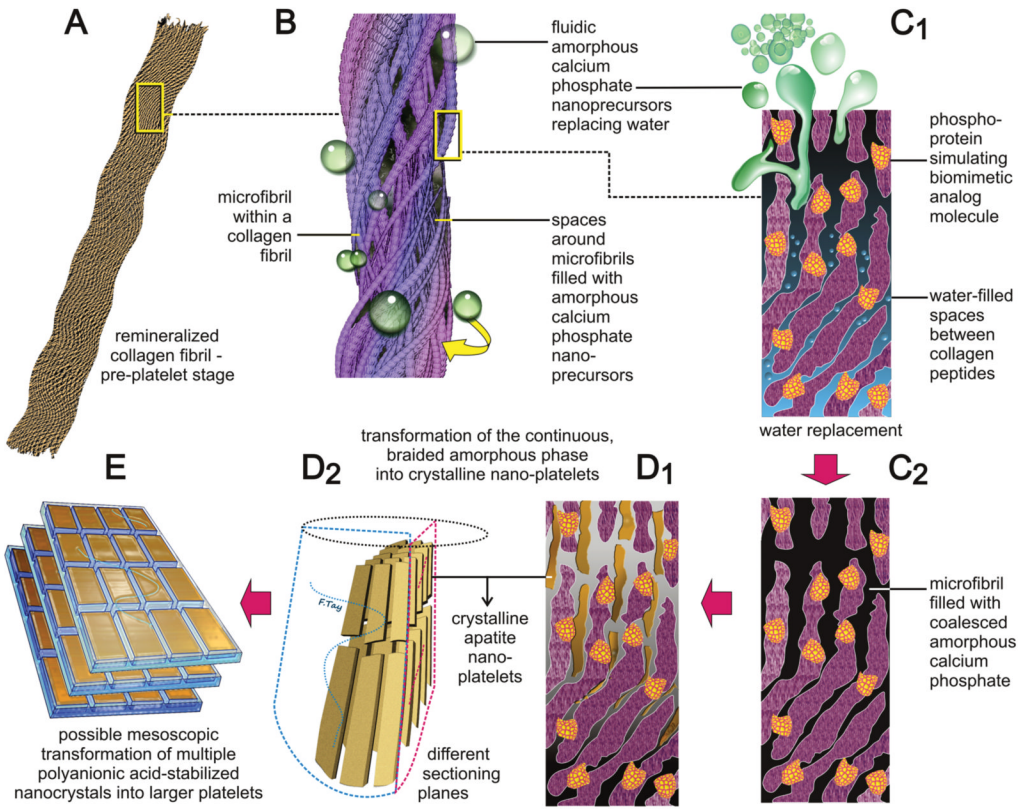

Scheme 1.

A schematic summarizing the features of biomimetic intrafibrillar remineralization observed in the completely-demineralized resin-infiltrated collagen matrices created in human dentin. **A**. Demineralized collagen fibril. **B**. Rope-like microfibril infiltrated with fluidic amorphous calcium phosphate droplets generated by the biomimetic remineralization system. **C1**. A view of a microfibril at the molecular level. Amorphous calcium phosphate infiltrating the spaces around the collagen molecules via capillary action. **C2**. Coalescence of the amorphous calcium phosphate in the microfibril. **D1, D2**. Transformation of continuous braided amorphous precursor into nanocrystals and their assembly into metastable mesocrystals. **E**. Hypothetical fusion of mesocrystals into larger, single crystalline platelets.